Modified emission of semiconductor nano-dots in three-dimensional photonic crystals

A.Z. Khokhar, R.M. De La Rue and N.P. Johnson

Abstract: Mono-dispersed polystyrene spheres were used to grow synthetic opal photonic crystals on glass substrates using controlled evaporation. Commercially available cadmium telluride (CdTe) semiconductor nano-dots with emission in the visible were infiltrated into a slice of opal voids by capillary action. The optical properties of CdTe dot loaded opal were studied by using a white light source and showed a red shift of the opal stop-band due to an increase in the effective refractive index. The emission of the CdTe dots was matched with the edge of the ⟨111⟩ direction stop-band of bare opal. Stop-band confined emission from CdTe dots was observed by pumping with an argon-ion laser. The full width at half maximum of the CdTe emission from an infiltrated section of the opal was significantly reduced due to the stop-band effect of bare opal.

1 Introduction

Semiconductor quantum dots (QDs), or nano-dots, having particle sizes on the order of a few nanometres have recently attracted considerable attention from a scientific as well as from an engineering point of view. The emission and absorption properties of these QDs can be tuned by varying their particle size [1] and also the material from which they are made [2]. Fluorescent emission from semiconductor QDs has advantages over dyes (such as R6G) since, after excitation, dyes only fluoresce for a small period of time that is a fraction of a second, and bleach within minutes or hours. On the other hand, QDs have longer fluorescence lifetimes. Semiconductor nano-dots embedded in photonic crystals (PhCs) therefore become a potentially interesting light source for optoelectronics applications.

There are two general approaches for the fabrication of three-dimensional (3D) PhCs: the top-down [3, 4] and bottom-up [5, 6] approaches. The bottom-up approach is potentially easier and less expensive. By using a bottom-up approach we have fabricated 3D synthetic opal from polystyrene spheres that exhibits a face-centred cubic structure. Such opal can be designed to work in the visible regime, with a stop-band in the $\Gamma-L$ direction, namely ⟨111⟩ [7].

In the last decade, various groups have studied the stop-band behaviour of light sources embedded in PhCs, for example R6G dye molecules and semiconductor nano-dots inside synthetic opal. QDs have been created in situ by using the vapour flow method [8], electrophoretic deposition [9] and also by slow evaporation of solutions [10].

Here we report cadmium telluride (CdTe) QDs infiltrated into synthetic opal by using capillary action. QDs in solution were allowed to dry in the voids of the opal. CdTe nano-dots were obtained from the American Dye Solution (ADS) company. The fluorescent emission of the CdTe dots peaked at 540 nm when excited at 457.9 nm. Synthetic opal was therefore fabricated with a stop-band centred at 555 nm and the reflectivity was measured, after infiltration of the QDs into the voids of the opal, by using a tungsten light source and a spectrometer. The stop-band was red-shifted because incorporation of the QDs caused increases in the effective refractive index of the composite. To observe fluorescent emission, the composite material (i.e. bare opal with CdTe) was excited using an Ar-ion laser and the emission of the QDs modified by the stop-band of the opal was observed.

2 Synthesis of polystyrene spheres

The polystyrene spheres were made by using surfactant-free emulsion polymerisation [11]. The reagents used were styrene (Aldrich 99%), potassium persulphate (Aldrich 99%) and de-ionised water. The styrene was distilled twice prior to polymerisation to remove any traces of inhibitor that is 4-*tert*-butylcatechol. The polymerisation was carried out in an aqueous solution at 80°C for 12 h under a nitrogen atmosphere. The reaction mixture was agitated using an overhead stainless steel stirrer rotating at 350–550 rpm. Polystyrene spheres with mean diameters in the range from 180 to 325 nm were synthesised by using this method. Controlled variation of the mean diameter of the spheres produced by this approach can be achieved in various ways: alteration of reagent concentration, variation of stirrer speed, alteration of the reaction temperature and alteration of the reaction time [12]. In the present work, the sphere size was varied by changing the reagent concentration and also by varying the stirrer speed. In the first case, the concentration of styrene was varied from 0.2 to 0.5 mol l^{-1}. The concentration of potassium persulphate, which was small by comparison with that of the styrene monomer, was kept constant and the stirrer speed remained fixed at 350 rpm. It was found that a smaller styrene concentration gives a smaller sphere size. In the second case, the

© The Institution of Engineering and Technology 2007

doi:10.1049/iet-cds:20060295

Paper first received 2nd October 2006 and in revised form 5th March 2007

The authors are with the Department of Electronics and Electrical Engineering, University of Glasgow, Glasgow G12 8QQ, Scotland, UK

E-mail: a.khokhar@elec.gla.ac.uk

amount of styrene remained fixed that is 0.5 mol l^{-1} and the other reagent parameters also remained fixed, while the stirrer speed varied form 350 to 550 rpm. It was found that smaller spheres were obtained at 550 rpm than at 350 rpm. To obtain a mono-dispersed distribution, both the stirrer speed and the temperature should be kept constant throughout the synthesis, thus maintaining a uniform rate of reaction. Transmission electron microscopy was used for size measurements, with at least 200 individual spheres being measured and the standard deviation was found to be 4%.

3 Fabrication of synthetic opal

The fabrication of synthetic opal was performed on a glass substrate using capillary growth of 230 nm diameter polystyrene spheres [13]. The glass substrate was cleaned with acetone, methanol, de-ionised water and blown dry with nitrogen gas. The spheres were dispersed in de-ionised water and a glass substrate was placed at an angle of 65° in a small vial, which was kept in a temperature-controlled environment. The temperature was set at 46°C and the relative humidity varied between 5 and 10%. After a week of exposure to this environment, the sample was found to have dried out and a 40–60 μm thick opal film of 230 nm polystyrene spheres was produced, with an average domain size of 70 μm. These films were found to be mechanically stable.

4 Infiltration of CdTe dots

The CdTe dots, as received from ADS, were dispersed in water. The CdTe dots were mono-dispersed having a particle size of 3.5 nm. They were infiltrated into the voids of the opal by using the capillary forces. The synthetic opal was blown with compressed nitrogen gas to remove domains that were not well attached to the substrate, before infiltration. The glass substrate with synthetic opal formed on it was placed in a small vial tilted an angle of 65° to the horizontal containing 2–3 ml of CdTe dots dispersed in water. A second blank glass substrate of the same size was placed directly on top (i.e. (111) plane) of the synthetic opal covered substrate, loosely touching the spheres [13]. Experiments were carried out both with and without a para-film acting as a spacer. Para-film thickness was 127 μm. This arrangement gave a sandwich or cell structure with a thin opal film between the two glass substrates. The colour of the thin opal film then changed rapidly (within a minute) due to infiltration of the CdTe dot solution into the voids of the opal. For slow evaporation of the solution, the vial was loosely capped and kept in the temperature-controlled environment. The temperature was set at 23°C and the relative humidity was varied from 25 to 30%. After two weeks of exposure in this environment, the sample was completely dry. The top substrate was removed carefully and the sample was observed in both optical and scanning electron microscopes (SEMs). It was found that good infiltration could be obtained when the top glass substrate was placed on the (111) plane of the synthetic opal, with a para-film spacer. However, a sample without the para-film spacer could be infiltrated only through the bottom 3 or 4 layers of the synthetic opal. Fig. 1 shows an optical micrograph of the thin film (Fig. 1*a*) before and (Fig. 1*b*) after infiltration of the CdTe QDs. In reflection, the opal thin film changed colour from green to red. This change in colour is attributable to an increase in the effective refractive index of the

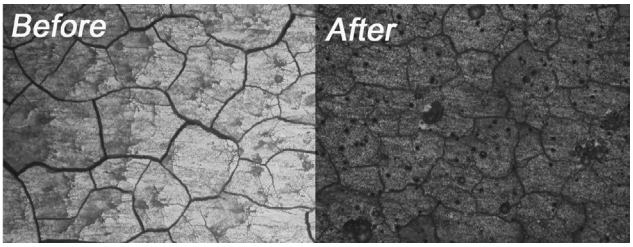

Fig. 1 *Optical micrograph before and after infiltration of CdTe QDs in voids of the opal*

Colour of thin film changed due to increase in the effective refractive index

composite. Fig. 2 shows SEM images of the thin film (Fig. 2*a*) before and (Fig. 2*b*) after infiltration of the CdTe dot solution. Cross-sections of the domains were also observed in the SEM. Fig. 2*c* shows good infiltration into a crystal thickness of 40 μm, while Fig. 2*d* also shows the formation of CdTe nano-pillars, as marked by the circle in the figure. These pillars are clearly formed between the domains of the opal thin film during the infiltration and drying process. (Note that Figs. 1 and 2 are taken from a sample that was infiltrated using a para-film spacer). The SEM micrograph of Fig. 3 was taken from a sample that had been infiltrated without using a para-film spacer. The inset (Fig. 3) shows the interface of the bare opal with the bottom layers, which are completely masked by the CdTe nano-dot in-fill.

5 Optical properties

5.1 Reflection measurements

To observe the changes in the optical properties, reflection measurements were made, both before and after the infiltration of the CdTe nano-dots. The sample with a high level of infiltration (i.e. completely in-filled) with CdTe was mounted on a rotating stage and was illuminated with a beam spot-size of 1 mm^2, using monochromated white light. The reflected light was detected using a silicon detector followed by a lock-in amplifier. The reflectance

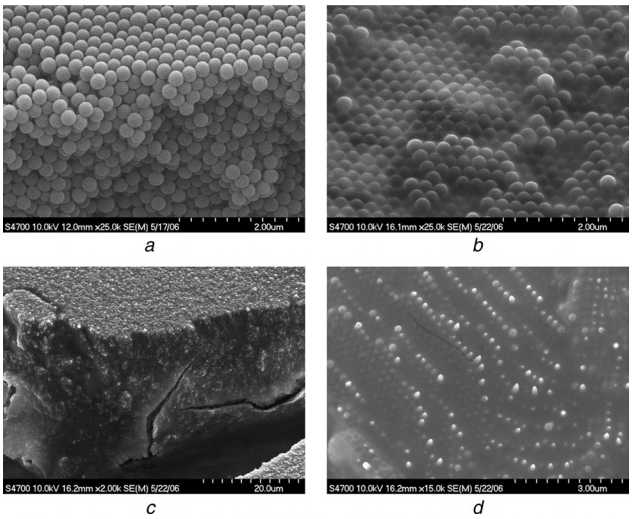

Fig. 2 *SEM images of thin film before and after infiltration of CdTe QDs*

a Bare synthetic opal
b (111) plane of synthetic opal after infiltration of CdTe QDs
c ~40 μm thick domain loaded with CdTe QDs
d Nano-pillars made of CdTe, observed between the domains

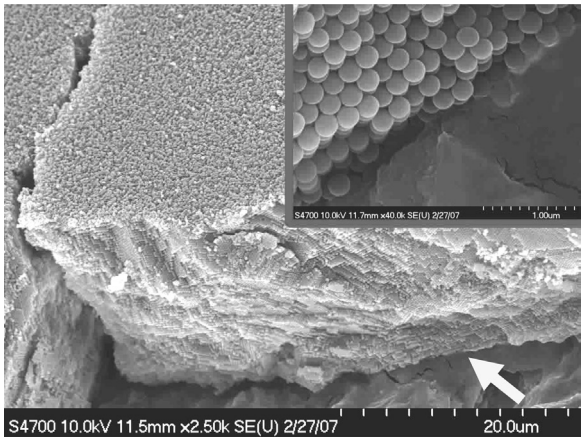

Fig. 3 *SEM image of thin film with few bottom layers completely masked by CdTe (indicated by arrow in the figure)*
Inset shows interface between the masked CdTe layers and bare opal

measurements were made at various angles of incidence. Fig. 4 shows normalised reflectance measurements before and after infiltration. A red shift in the reflectance measurements is observed due to changes in the value of n_{eff}. By altering the angle of incidence (θ), the effective refractive index (n_{eff}) and inter-planar spacing (d) could be determined [14]. The plot of λ^2 against $\sin^2\theta$ shown in Fig. 5 gives a straight line with its y-intercept equal to n_{eff}^2 and a slope of $1/4d^2$, where λ is the peak stop-band wavelength. From Fig. 5, n_{eff} is found to have increased from 1.46 to 1.58.

5.2 Photoluminescence measurements

The CdTe QDs gave fluorescent emission at 540 nm when excited at near-normal incidence with a 457.9 nm wavelength Ar-ion laser. For the photoluminescence experiments a sample was selected with a few bottom layers (i.e. 3 or 4 layers) infiltrated with the CdTe that is the emission of the CdTe nano-dots was matched to the short-wavelength edge of the stop-band of the bare opal. From Fig. 3 it was found that the bottom 3 or 4 layers are completely covered by the CdTe dot in-fill and the remaining layers (i.e. more than 100 layers) are unfilled. These bottom layers covered by the CdTe nano-dot in-fill have

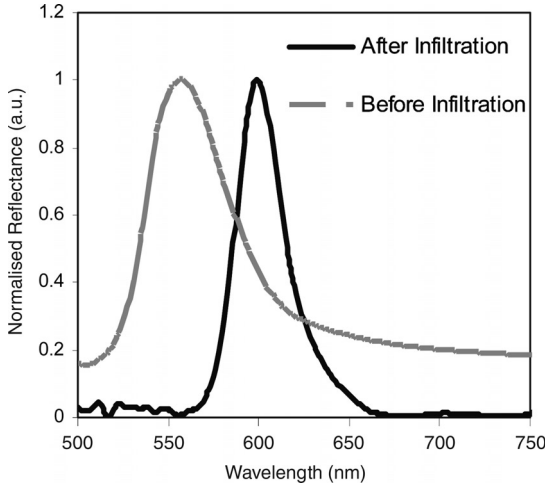

Fig. 4 *Normalised reflectance measurements before and after infiltration of CdTe QDs*
Red shift was observed due to increase in the effective refractive index

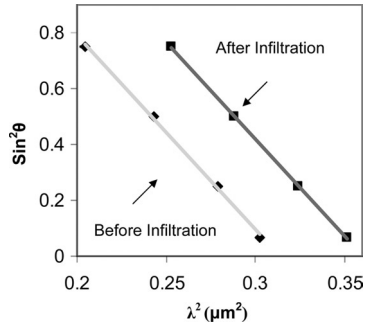

Fig. 5 *Plot of square of reflectance maxima against $\sin^2\theta$*
After the infiltration, the effective refractive index contrast increased

no stop-band effect that is they are spectrally featureless as the spheres are substantially masked by the CdTe dot in-fill (see the inset of Fig. 3). A sample was excited at normal incidence to the (111) plane of the bare opal. The excitation power was set at 340 mW, with a spot size of 2 mm. The optical emission was collected from the (111)-oriented surface of bare opal by using a spherical lens, and coupled into a fibre-optic cable connected to a spectrometer. Fig. 6 shows the emission spectrum of the CdTe dots in the synthetic opal. The sample was also rotated slightly with respect to the excitation beam, which modified the emission. The observed modification in the emission is attributable to the presence of the stop-band edge of the synthetic opal. An indication of the long-term stability of the emission was obtained from the observation that the intensity of the emission remained constant for 1 h, at an excitation power of 1.8 W. To see more clearly the effect of the stop-band of the loaded opal on the emission spectrum, the measured spectra of Fig. 6 were then normalised with respect to a background spectrum consisting of a thin layer of CdTe dot solution deposited and dried out on a glass substrate, as shown in Fig. 7. Fig. 7 shows the intensity ratio of the spectrum after this normalisation. From Fig. 7 it can be seen that the emission of the CdTe dots is indeed close to the short-wavelength edge of the stop-band of bare-opal. It was found that the peak of this emission could be tuned from 543 to 551 nm

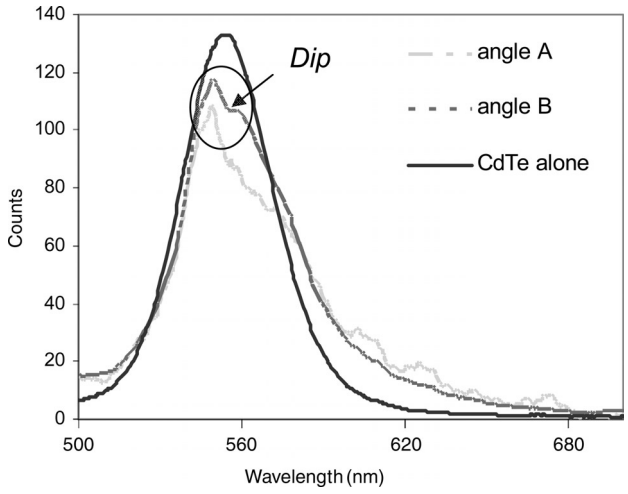

Fig. 6 *Fluorescence emission spectra of CdTe QDs embedded in the synthetic opal as marked by circle*
Emission was modified due to the stop-band as indicated by dip
Angle '*B*' is normal incidence (i.e. 0°) whereas angle '*A*' is 15°. 'CdTe alone': spectrum from the CdTe thin layer deposited on the glass substrate used as a background spectrum

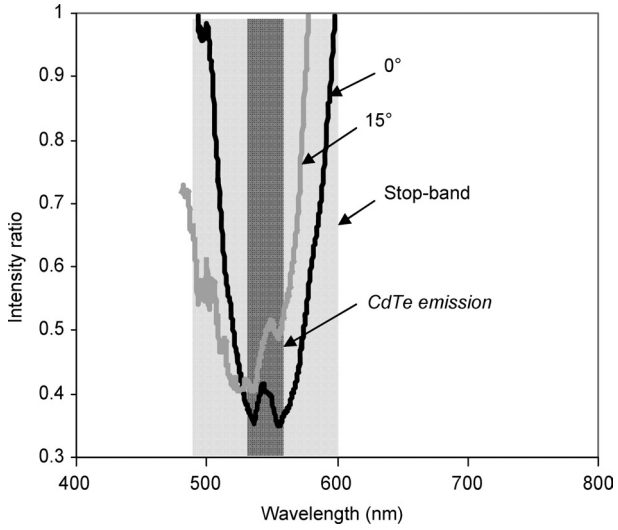

Fig. 7 *Intensity ratios of the fluorescence emission of the CdTe*

The spectra are obtained by dividing the modified emission (as shown in Fig. 6) by the background spectrum. The shaded area indicates the stop-band which is shifted towards the shorter wavelength by rotating the sample for 0° to 15°. The emission of CdTe is also shown and FWHM is reduced to 11 nm due to the emission suppressed by the stop-band

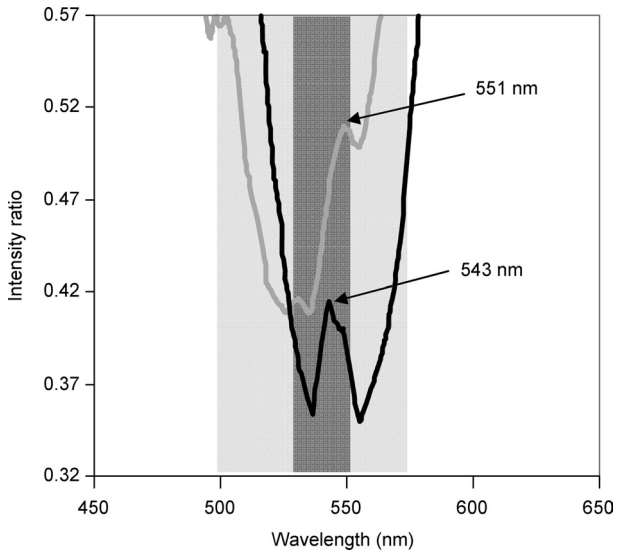

Fig. 8 *Magnified view of Fig. 7*

by slightly rotating the sample, as shown in Fig. 8. That is, by changing the angle of incidence of the excited beam away from the normal, the stop-band was shifted towards shorter wavelengths, and the emission of the QDs changed its position accordingly. It was also found that the full width at half maximum (FWHM) of the CdTe dot emission was significantly reduced by the stop-band of bare opal. From Figs. 7 and 8, we have calculated that the FWHM of the CdTe dot emission changed from 40 to 11 nm in the synthetic opal. However, no decrease in line width was observed as the excitation beam power was increased from 340 mW to 1.8 W.

6 Discussion and conclusion

In this paper, we report on a simple and inexpensive technique for the infiltration of semiconductor CdTe nanoparticles in the voids of the opal. The technique is based on capillary action, together with slow evaporation of the solution in the voids of the opal. SEM images show a high level of infiltration. The emission of the CdTe dots is at 540 nm when excited with 457.9 nm, which is matched with the stop-band edge of the synthetic opal. From the optical reflectivity it was found that the stop-band of the synthetic opal was shifted towards the longer wavelengths. The shift was found due to an increase in the value of n_{eff}. The n_{eff} is of the synthetic opal changed from 1.46 to 1.58 after infiltration of the CdTe nano-dots. The emission of the CdTe in the synthetic opal was also studied by exciting the sample with the 457.9 nm wavelength of an Ar-ion laser. The emission of the CdTe was modified by the stop-band of the bare opal. In this case, the band-edge emission from the CdTe in the stop-band was studied. The FWHM of the CdTe dot emission was reduced from 40 to 11 nm in the synthetic opal. The emission observed from the CdTe dots was also tuned by rotating the sample with respect to the normal incidence angle of the excited beam. Such a change in the FWHM of the CdTe emission is encouraging and should be helpful in fabricating lasers using the distributed feedback mechanism, for applications in optoelectronics.

On the basis of our results we believe that lasing emission from CdTe nano-dots embedded in synthetic opal is possible if two criteria are fulfilled. First, the crystal should be sufficiently thick (~1 mm) to provide the distributed feedback mechanism [15] along the (111) direction normal to the film plane over a sufficient distance. Secondly, the refractive index of the CdTe nano-dots, embedded in an in-fill matrix, should be matched with that of synthetic opal [16]. Perfect matching of the index of the potential laser host material with the synthetic opal makes the sample semi-transparent and irridescent. This combination should make it possible to amplify the spontaneous emission of a distributed light source embedded in the synthetic opal. Bulk CdTe has a refractive index around 2.8 at optical frequencies [17]. In the context of the present work, the refractive index of the deposited CdTe QDs is therefore much higher than the refractive index of the polystyrene spheres, which is 1.59 and cannot be matched. However, an inverse structure of TiO_2 could possibly be matched to a close approximation.

7 Acknowledgment

The authors acknowledge support from the 'Metamorphose' Network of Excellence.

8 References

1 Rogach, A.L.: 'Nanocrystalline CdTe and CdTe (S) particles: wet chemical preparation, size-dependent optical properties and perspectives of optoelectronic applications', *Mater. Sci. Eng. B*, 2000, **69–70**, pp. 435–440
2 Eychmüller, A., and Rogach, A.L.: 'Chemistry and photophysics of thiol-stabilized II–VI semiconductor nanocrystals', *Pure Appl. Chem.*, 2000, **72**, (1–2), pp. 179–188
3 Subramania, G., and Lin, S.Y.: 'Fabrication of three-dimensional photonic crystal with alignment based on electron beam lithography', *Appl. Phys. Lett.*, 2004, **85**, (21), pp. 5037–5039
4 Campbell, M., Sharp, D., Harrison, M.T., Denning, R.G., and Tuberfield, A.J.: 'Fabrication of photonic crystals for the visible spectrum by holographic lithography', *Nature*, 2003, **404**, pp. 53–56
5 Blaaderen, A.V.: 'Opals in a new light', *Science*, 1998, **282**, pp. 887–888
6 Jin, C., McLachlan, M.A., McComb, D.W., De La Rue, R.M., and Johnson, N.P.: 'Template-assisted growth of nominally cubic

(100)-oriented three-dimensional crack-free photonic crystals', *Nano Lett.*, 2005, **5**, (12), pp. 2646–2650
7 Reynolds, A., López-Tejeira, F., Cassagne, D., García-Vidal, F.J., Jouanin, C., and Sanchez-Dehesa, J.: 'Spectral properties of opal-based photonic crystals having a SiO_2 matrix', *Phys. Rev. B*, 1999, **60**, pp. 11422–11426
8 Vlasov, Yu.A., Luterova, K., Pelant, I., Hönerlage, B., and Astratov, V.N.: 'Enhancement of optical gain of semiconductors embedded in three-dimensional photonic crystals', *Appl. Phys. Lett.*, 1997, **71**, (12), pp. 1616–1618
9 Rogach, A.L., Kotov, N.A., Koktysh, D.S., Ostrander, J.W., and Ragoisha, G.A.: 'Electrophoretic deposition of latex-based 3d colloidal photonic crystals: a technique for rapid production of high-quality opals', *Chem. Mater.*, 2000, **12**, pp. 2721–2726
10 Vlasov, Y.A., Yao, N., and Norris, D.J.: 'Synthesis of photonic crystals for optical wavelengths from semiconductor quantum dots', *Adv. Mater.*, 1999, **11**, (2), pp. 165–169
11 Goodall, A.R., Hearn, J., and Wilkinson, M.C.: 'The preparation and characterisation of monodisperse polystyrene lattices – using potassium peroxydiphosphate free radical initiator', *Br. Polym. J.*, 1978, **10**, pp. 141–150
12 Madaeni, S.S., and Ghanbarian, M.: 'Characterization of polystyrene latexes', *Polym. Int.*, 2000, **49**, pp. 1356–1364
13 McLachlan, M.A., Johnson, N.P., De la Rue, R.M., and McComb, D.W.: 'Thin film photonic crystals: synthesis and characterisation', *J. Mater. Chem.*, 2004, **14**, pp. 144–150
14 Johnson, N.P., McComb, D.W., Richel, A., Treble, B.M., and De la Rue, R.M.: 'Synthesis and optical properties of opal and inverse opal photonic crystals', *Synth. Met.*, 2001, **116**, pp. 469–473
15 Shkunov, M.N., Vardeny, Z.V., DeLong, M.C., Polson, R.C., Zakhidov, A.A., and Baughman, R.H.: 'Tunable, gap-state lasing in switchable directions for opal photonic crystals', *Adv. Funct. Mater.*, 2002, **2**, (1), pp. 21–26
16 Frolov, S.V., Vardeny, Z.V., Zakhidov, A.A., and Baughman, R.H.: 'Laser-like emission in opal photonic crystals', *Opt. Commun.*, 1999, **162**, (4–6), pp. 241–246
17 Palik, E.D.: 'Handbook of optical constants of solids' (Academic Press Limited, 1998), p. 1